SDSMT/IAS/R-91/04

August 1991

A CLOUD, PRECIPITATION AND ELECTRIFICATION MODELING EFFORT FOR COHMEX

By: Harold D. Orville, John H. Helsdon, and
Richard D. Farley, Principal Investigators

Prepared for:

National Aeronautics and Space Administration
George C. Marshall Space Flight Center
Marshall Space Flight Center, AL 35812

Final Technical Report on Grant No. NAG 8-632
Period Covered: 20 May 1987 - 19 May 1991

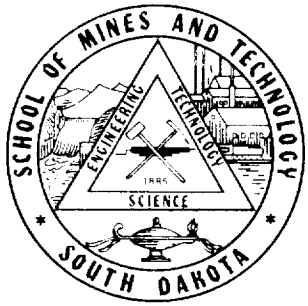

Institute of Atmospheric Sciences

South Dakota School of Mines and Technology

501 E. St. Joseph Street

Rapid City, South Dakota 57701-3995

SDSMT/IAS/R-91/04

August 1991

A CLOUD, PRECIPITATION AND ELECTRIFICATION MODELING EFFORT FOR COHMEX

By: Harold D. Orville, John H. Helsdon, and
Richard D. Farley, Principal Investigators

Prepared for:

National Aeronautics and Space Administration
George C. Marshall Space Flight Center
Marshall Space Flight Center, AL 35812

Final Technical Report on Grant No. NAG 8-632
Period Covered: 20 May 1987 - 19 May 1991

Institute of Atmospheric Sciences

South Dakota School of Mines and Technology

501 E. St. Joseph Street

Rapid City, South Dakota 57701-3995

TABLE OF CONTENTS

LIST OF FIGURES

LIST OF TABLES

1. INTRODUCTION

The Modeling Group of the Institute of Atmospheric Sciences (IAS) began in mid-1987 to simulate and analyze cloud runs that had been made during the COHMEX project and later. Our cloud model had been run nearly every day by Fred Kopp during the summer 1986 COHMEX project. The Modeling Group was then funded to analyze the results, make further modeling tests, and help explain the precipitation processes in the southeastern United States.

The main science objectives of COHMEX were:

1) To observe the pre-storm environment and understand the physical mechanisms leading to the formation of small convective systems and processes controlling the production of precipitation.

2) To describe the structure of small convective systems producing precipitation including the large and small scale events in the environment surrounding the developing and mature convective system.

3) To understand the interrelationships between electrical activity within the convective system and the process of precipitation.

4) To develop and test numerical models describing the boundary layer, tropospheric and cloud scale thermodynamics and dynamics associated with small convective systems.

The latter three of these objectives were addressed by the modeling activities of the IAS. We used a series of cloud models to simulate the clouds that formed during the operational project. The primary models used to date on the project have been a two-dimensional (2D), bulk water model, a two-dimensional electrical model, and to a lesser extent, a two-dimensional, detailed microphysical cloud model. Unfortunately, no three-dimensional runs have been made during the time period of this grant. All of the models are based on fully interacting microphysics, dynamics, thermodynamics, and electrical equations.

Only the 20 July 1986 case has been analyzed in detail, although all of the cases run during the summer have been analyzed as to how well they did in predicting the characteristics of the convection for the day. Even though the funding support for the study is over, the model results are still being analyzed and papers will still be published, with partial credit being given to the NASA grant.

2. PRINCIPAL RESULTS

The results can be categorized as to 1) forecasting capabilities of the models; 2) studies of the precipitation processes in these small convective systems; and 3) studies of the primary electrical processes operating in the clouds in the southeastern region of the United States.

2.1 Forecast Capabilities

A two-dimensional, time-dependent cloud model was run in the morning before operations began using the rawinsonde data from Huntsville, Alabama. In addition, a

one-dimensional (1D), steady-state model was run on many of the soundings available from the project. Results were published in a thesis by James Jung and indicated that four conditions were necessary for these cloud models to be accurate as forecast tools.

1) The sounding must be representative of the forecast area.

2) The sounding must remain representative throughout the forecast time frame.

3) There can be no large scale forcing for the one-dimensional model tested here.

4) Water vapor and temperature advection changes should be small.

In addition, to forecast the occurrence of precipitation accurately at Huntsville, the cloud models must have cloud bases at or below 2.5 km and cloud tops higher than 6 km. Under these conditions, the 2D model was accurate in all of the 21 days on which it was run; and the 1D model, 85% of the 46 days it was run on. More data would be needed to confirm these results.

These models have often been used to predict cloud top height. In this case, they did not do so well. The 2D model had a correlation coefficient of 0.72 for convective days; the 1D model only 0.50. However, the maximum temperature prediction of the 2D model was quite good, being within 2.5°C of the observed maximum for 70% of the days (Kopp et al., 1990). A more complete manuscript reporting on the forecast capabilities of the 2D time-dependent cloud model has been submitted for publication (Kopp and Orville, 1991).

2.2 Precipitation Processes

2.2.1 Overview

The primary study illustrating the important precipitation processes in these warm base clouds is the one by Tuttle et al. (1989), published in the Journal of the Atmospheric Sciences. The 20 July 1986 case provided the data for the analysis by both multiparameter radar and by numerical modeling efforts. This was the first case that we know of in which a multidimensional, time-dependent cloud model was run in advance of the actual convection of the day. The early clouds on this day topped out between 6 and 8 km and contained little ice. The primary precipitation process was rain formed by coalescence. After about 45 minutes of this preliminary cloud and precipitation development, strong convection appeared. A rapidly growing cell broke through the moderate size cells, carried large drops into supercooled regions where freezing occurred, and stimulated further growth.

An analysis of the production terms (as shown in Figs. 1 and 2) for these types of storms reveals that the coalescence term initiates the precipitation and then accretion takes over to produce most of the rain. However, the melting of graupel is a close second, although occurring nearly 15 minutes later in the active large cell. The initiation of graupel occurred through the probabilistic freezing of rain. This is the only process which can initiate graupel/hail until snow and cloud ice are available. The snow melt and shedding terms also produced a small amount of rain.

The growth of graupel/hail, after their initiation, occurs primarily by the accretion of supercooled liquid water, both cloud and rain. The interaction of snow

and rain to form graupel is an important source for the graupel. If cloud ice were present at warmer temperatures, such as -5 to -10°C, then this also would cause graupel and snow formation through the interactions of rain with the cloud ice.

This case has also been run with all of the ice processes turned off. Eleven percent less precipitation was produced from a cloud cell that did not grow as high as the cell with ice in it (about 1.4 km difference in height). Additional runs were made. Different amounts of ice were simulated and the results indicated that there is an optimum amount of ice development to produce the most precipitation from a cloud, even though most of the precipitation was formed by coalescence and accretion. These ice studies also showed the critical influence that the dynamics of the cloud play in the production of precipitation. This relates to the production of snow or graupel and the ease with which the updrafts can carry the particles to the anvil. Less efficient precipitation occurs when more of the particles are spewed out the anvil, which will occur if the ice particles are mainly snow instead of graupel.

The major difference in the production of precipitation from this maritime sounding from the southeastern United States region and from the continental soundings in the Northern Plains is the predominant influence of the warm rain process in the maritime clouds. Even so, the ice processes play an important role, particularly in the more vigorous cells. These aspects are clearly illustrated by the following comparison of precipitation development for the two regions.

2.2.2 Comparison of Precipitation Development in the Northern High Plains and in the Southeastern United States

Two thoroughly studied cases form the basis for the comparison. One case is the August 1, 1981 CCOPE case from the Montana region and the other is the 20 July case from COHMEX. Figures 1 and 2 show the various terms that contribute to the production of rain and graupel/hail for the southeastern United States case. Figures 3 and 4, taken from Kubesh et al. (1988), show the same information for the High Plains case. First we will discuss the production of graupel/hail and then rain in the two cases.

Graupel/hail production terms:

1) Accretional growth and the melting of graupel/hail are the biggest terms -- exceeding 100 kT/km in both cases.

2) Wet growth of the graupel/hail (not shown) is 5 to 15% of accretional growth in both cases being larger in the COHMEX case.

3) Graupel accreting snow is an important term in both areas (>50 kT/km).

4) Rain/snow interactions are important in the COHMEX case (a total of 70 kT/km) and of order 30 kT/km in the CCOPE case.

5) Cloud ice/rain interactions are more important in the High Plains (2.5 kT/km) than in the Southeast (0.1 kT/km).

6) The probabilistic (Bigg) freezing of rain is a significant early source of graupel/hail in the COHMEX case with high coalescence amounts, but totals less than 0.5 kT/km in both cases.

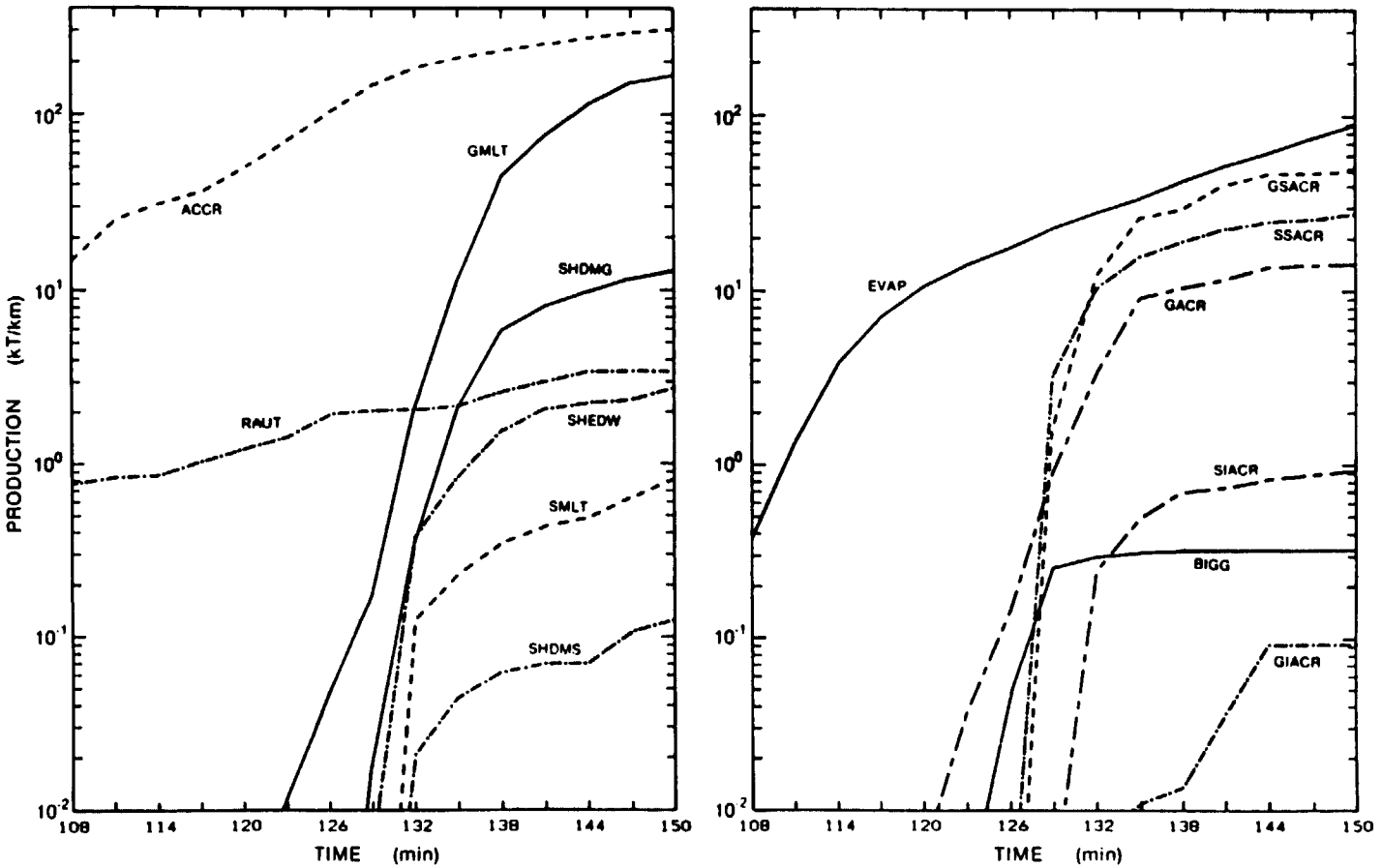

Fig. 1: Rain production due to the processes listed for the bulk model simulation of the 20 July COHMEX case. Processes contributing to a gain(loss) in the rain field are shown in the left (right) pannel. The units of production are kT km^{-1}. The curves are the result of the various rates being summed over the entire domain and accumulated to the indicated time.

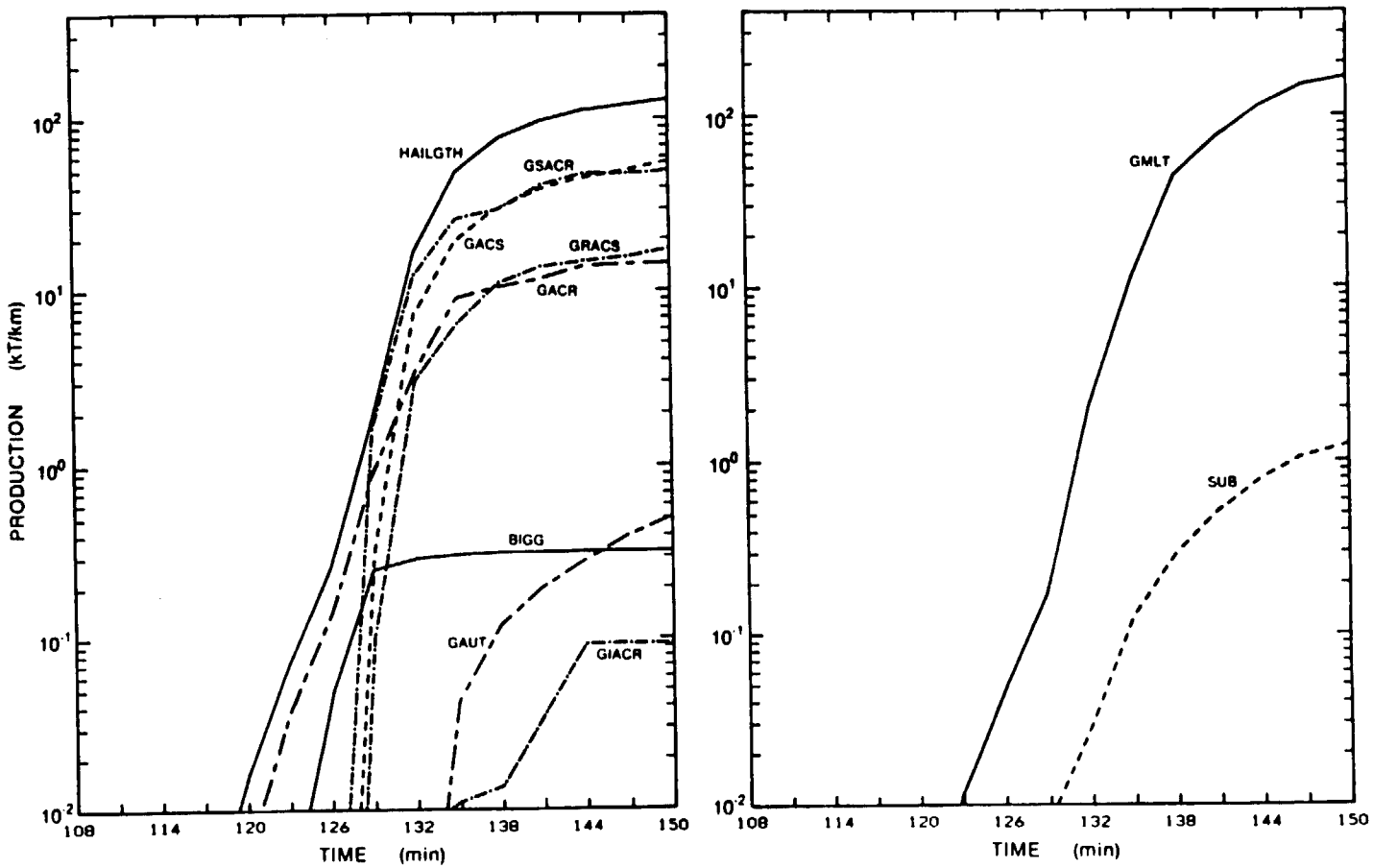

GENERATION MECHANISMS
GAUT=Graupel/hail formed by autoconversion (aggregation) of snow.
GRACS=Accretion of snow by rain, forming graupel/hail.
GSACR=Accretion of rain by snow, forming graupel/hail.
GIACR=Accretion of rain by cloud ice, forming graupel/hail.
BIGG=Probabilistic freezing of rain to form graupel/hail.

GROWTH MECHANISMS
HAILGTH=Total accretional growth of graupel/hail.
GACS=Accretion of snow by graupel/hail.
GACR=Accretion of rain by graupel/hail.

LOSS MECHANISMS
GMLT=Loss of graupel/hail by melting to form rain.
SUB=Loss of graupel/hail by sublimation.

Fig. 2: As in Fig. 1, except for the graupel/hail field.

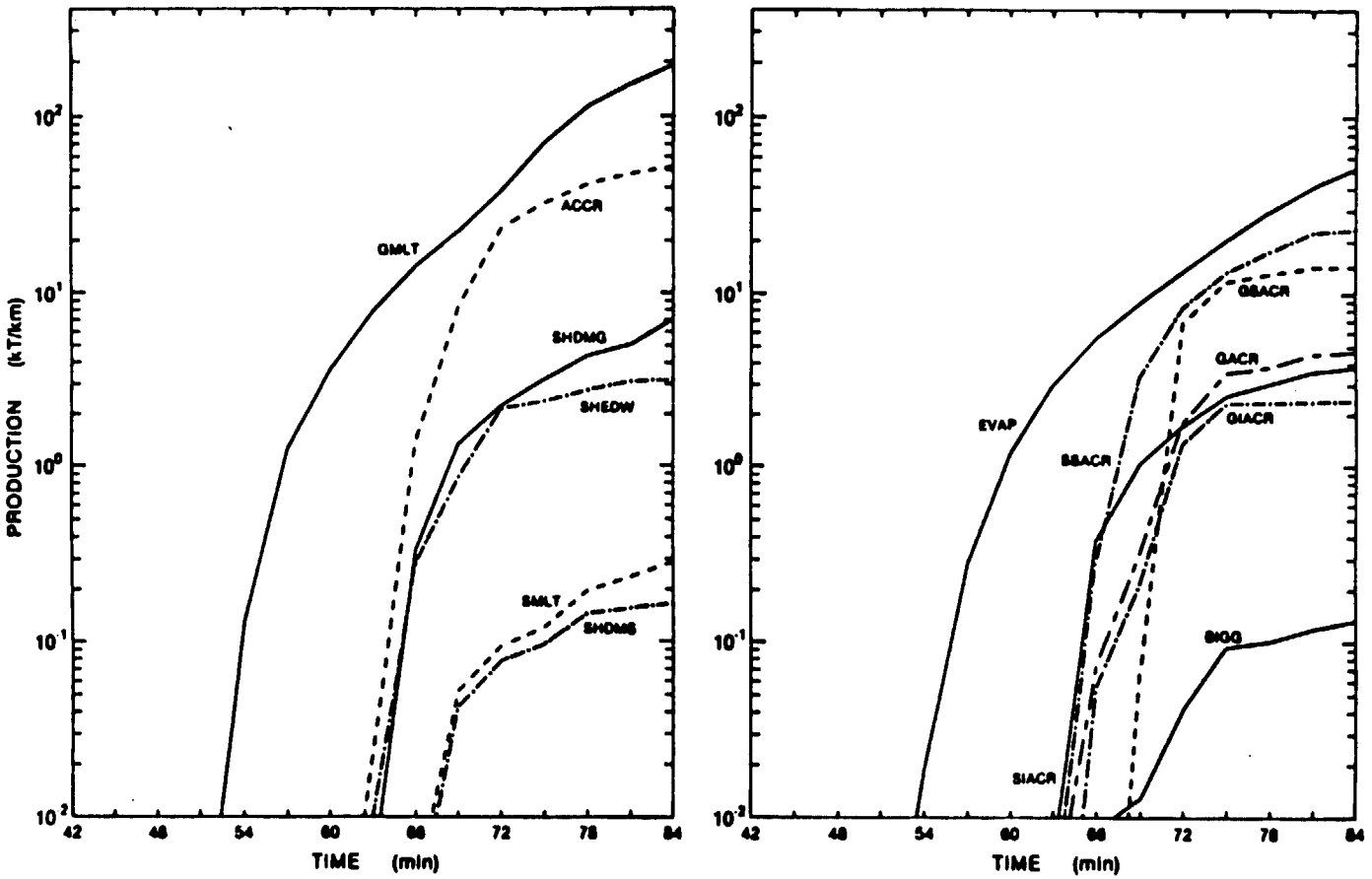

GENERATION/GROWTH MECHANISMS
RAUT=Rain formed by autoconversion of cloud water.
GMLT=Rain formed by melting of graupel/hail.
SMLT=Rain formed by melting of snow.
SHEDW=Rain from shedding during wet growth of graupel/hail.
SHDMG=Rain from shedding during melting of graupel/hail.
SHDMS=Rain from shedding during melting of snow.
ACCR=Rain growth by accretion of cloud water.

LOSS MECHANISMS
EVAP=Evaporation of rain.
SIACR=Accretion of rain by cloud ice, forming snow.
SSACR=Accretion of rain by snow.
GACR=Accretion of rain by graupel/hail.
GSACR=Accretion of rain by snow, forming graupel/hail.
GIACR=Accretion of rain by cloud ice, forming graupel/hail.
BIGG=Probabilistic freezing of rain to form graupel/hail.

Fig. 3: As in Fig. 1, except for the 1 August CCOPE case.

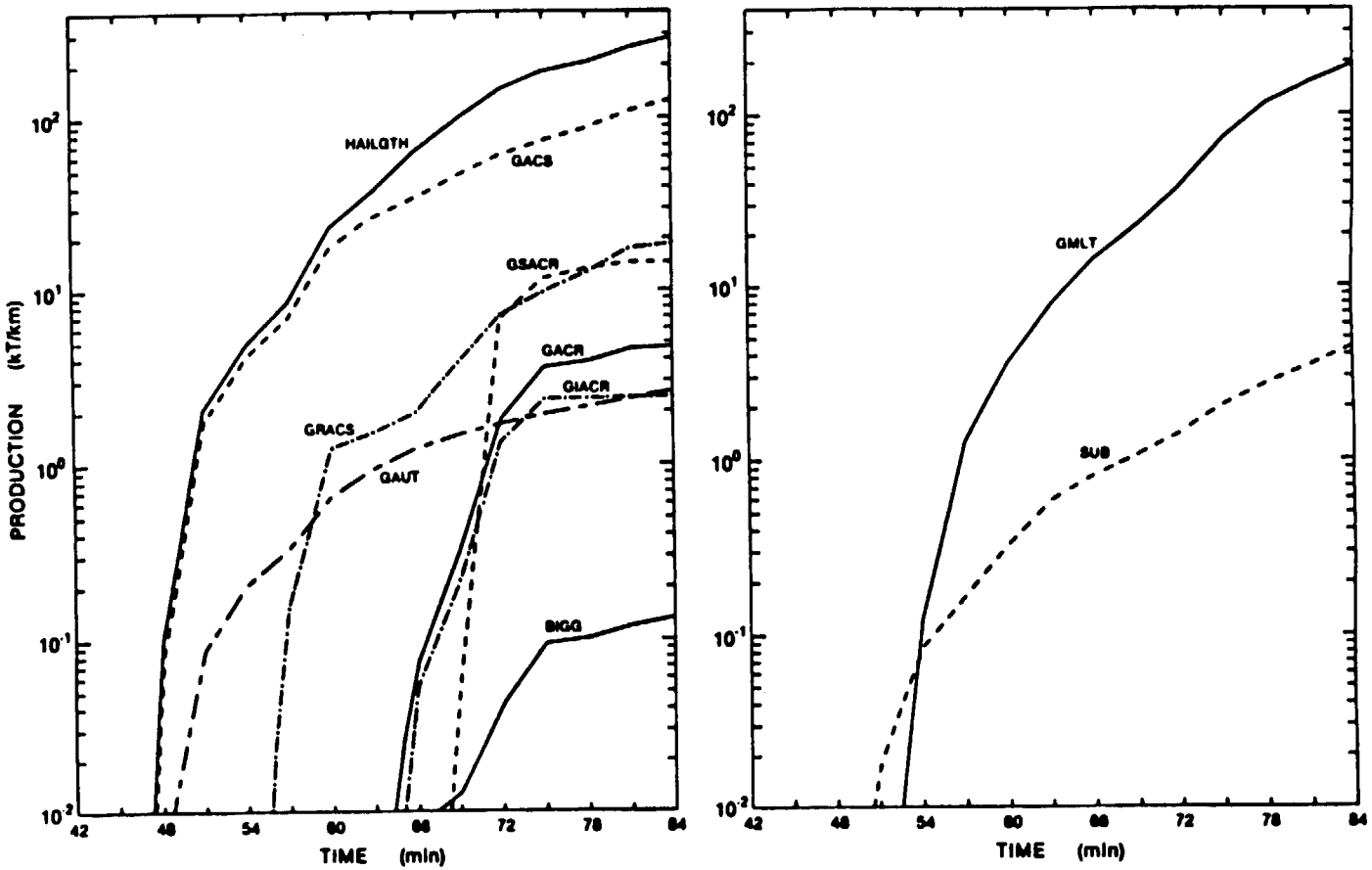

GENERATION MECHANISMS
GAUT=Graupel/hail formed by autoconversion (aggregation) of snow.
GRACS=Accretion of snow by rain, forming graupel/hail.
GSACR=Accretion of rain by snow, forming graupel/hail.
GIACR=Accretion of rain by cloud ice, forming graupel/hail.
BIGG=Probabilistic freezing of rain to form graupel/hail.

GROWTH MECHANISMS
HAILGTH=Total accretional growth of graupel/hail.
GACS=Accretion of snow by graupel/hail.
GACR=Accretion of rain by graupel/hail.

LOSS MECHANISMS
GMLT=Loss of graupel/hail by melting to form rain.
SUB=Loss of graupel/hail by sublimation.

Fig. 4: As in Fig. 2, except for the 1 August CCOPE case.

7) Sublimation is of the same order in both cases (1 kT/km).

Rain production terms:

1) Melting of graupel/hail is the biggest term in CCOPE (200 kT/km), and accretion the biggest term in COHMEX (300 kT/km). However, melting approaches 170 kT/km in COHMEX. Hence, both storms produce similar amounts of rain through the ice processes. COHMEX produces additional rain via coalescence.

2) The time of ice production is similar in the two cases, about 30 minutes, and some of the quantities are of the same magnitude.

3) Evaporation is greatest in the COHMEX case (90 vs. 50 kT/km).

4) Rain/snow interactions result in approximately 80 kT/km loss of rain to graupel or snow in COHMEX; less than 50% of this in the CCOPE case.

5) Shedding during wet growth is low in both cases (3 kT/km). Shedding during melting of graupel is of order 10 in both cases. Shedding from melting snow is of order 0.1 kT/km.

6) Accretion is the second largest term in CCOPE (50 kT/km); the largest term in COHMEX.

7) Autoconversion (coalescence) is about 3.5 kT/km in COHMEX, and is deactivated in CCOPE.

2.2.3 Comparison of Models of Differing Microphysical Detail

The two-dimensional hail category model, which partitions the precipitating ice field into 20 logarithmically spaced size categories, has also been run on the 20 July COHMEX case. This model employs a more detailed and realistic treatment of the growth and sedimentation of ice in the simulated clouds and facilitates more detailed studies of the growth of ice. Comparison of the results of the detailed model with results of the bulk model also allows assessment of the relative adequacy of the bulk model's treatment of ice in various situations.

For the 20 July COHMEX case, the results of the two models show a high degree of similarity over the duration of the simulations, especially in terms of large scale structure, dynamic features, and evolution. Microphysical aspects, whether in terms of maximum values or domain totals, also display similarities throughout, even though ice is treated quite differently in the two models. This is due to the dominant role of the warm rain process (which is treated similarly in the two models) in maritime situations such as this COHMEX case. Although specific aspects of the production of precipitating ice, especially the contact freezing of rain, show pronounced differences for the two models, these aspects usually play a secondary role and exert minor influence compared to the dominant terms.

The growth of the precipitating ice field tends to be somewhat more continuous in the detailed model. This results in a single peak in the temporal evolution of the maximum values of precipitating ice content, whereas the bulk model indicates two strong peaks or bursts in the growth and development of graupel/hail. The period of intensive growth of the precipitating ice for the detailed model is preceded and followed by peaks in maximum rain contents, whereas the two peaks in rain are

correlated with the two graupel/hail peaks for the bulk model. The detailed model clearly indicates that most of the precipitating ice is in the form of graupel, usually a factor of two or more greater than the amount of hail.

The most striking difference in the results of the two models is the estimated radar reflectivity factor with a maximum of just under 73 dBz indicated for the bulk model versus a maximum of 63 dBz for the detailed model. Another obvious difference between the two models is the amount of hail at the surface, with the bulk model indicating a factor of two to three times more hail than the detailed model, although the vast majority of the surface precipitation is in the form of rain.

Table 1 is a compilation of some of the differences in the predictions of the bulk and detailed models for this particular COHMEX case. Also included in the table are the results for another maritime case (Wallops Island) and three continental cases (Alberta, CCOPE 2 August, and CCOPE 1 August). The two models display more pronounced differences for the continental cases with precipitation development being more efficient in the bulk model.

2.2.4 Microbursts

Another aspect of our modeling studies has concentrated on the factors influencing the formation and strength of the microbursts which are frequently seen in our simulations. The simulations of the 20 July COHMEX case also produce microbursts, a weak microburst forced solely by rain in the early stages and a period of intense microburst activity associated with the late mature and dissipating stage of the major storm cell of the simulations. Close examination of this 15-minute period of intense microburst activity revealed the presence of two microbursts, with the second and slightly stronger microburst superimposed on the expanding outflow of the first. These two microbursts were forced by the fallout of the two disinct precipitation cores (primarily rain) noted above. The primary forcing mechanism for these microbursts was the evaporation of rain. The most intense portions of these microbursts were due to additional forcing from the melting of graupel/hail. Studies of the trajectories of air parcels that ended up in the outflow revealed that most of the parcels originated at elevations below 3 kilometers.

The results of the 20 July COHMEX case have also been used to expand the number of cases used in developing an index for describing and possibly forecasting microbursts. This "microburst index" is based on the combined effects of precipitation loading, melting, and evaporation as quantified by the model results. Evaporation and melting are, in general, the most dominant effects. Values of a few degrees per minute cooling occur in the stronger microburst cases. The heights of the melting level and the cloud base (for the start of evaporation) and the depth of the precipitation shaft are key factors which enable the microphysical processes to act over longer or shorter time periods. The microburst index based on these combined effects has been determined for a number of different cases from various geographic regions which produce a wide range of microbursts -- some very wet and some nearly dry. Results to date indicate a correlation coefficient of 0.88 between the microburst index and the maximum divergence indicated in the model results.

2.3 Atmospheric Electrical Processes

The Storm Electrification Model (SEM) of Helsdon et al. (1984) and Helsdon and Farley (1987a,b) was used to study the electrical development of the 20 July COHMEX storm. In previous work, this model has been used to study the

TABLE 1: COMPARISON OF MODEL RESULTS

QUANTITY		ALBERTA		CCOPE 2 AUG		CCOPE 1 AUG		WALLOPS ISLAND		COMHEX	
		BULK	DTLD	BULK	DTLD	BULK	DTLD	BULK	DTLD	BULK	DTLD
EXTREME VALUES											
Maximum Cloud Water	(g/kg)	4.6	5.0	8.9	9.3	8.5	9.0	5.1	5.2	4.4	4.7
Maximum Cloud Ice	(g/kg)	1.5	1.5	5.2	6.0	6.8	8.5	1.6	1.4	1.8	1.5
Maximum Rain	(g/kg)	5.6	5.9	6.9	6.6	7.1	4.4	11.2	11.1	13.1	13.3
Maximum Precipitating Ice	(g/kg)	7.0	10.8	10.9	12.5	10.9	9.4	14.1	13.5	11.1	10.9
Maximum Updraft	(m/s)	25.2	31.5	54.3	56.6	50.0	49.9	30.6	31.3	23.1	20.4
Maximum Downdraft	(m/s)	13.9	13.5	28.6	28.8	25.9	25.1	17.3	21.0	21.2	16.3
Maximum Reflectivity Factor	(dBz)	70.5	60.1	70.9	63.4	69.4	60.1	75.0	65.4	72.8	63.0
SURFACE PRECIPITATION CHARACTERISTICS											
Peak Rainfall	(mm)	25.6	29.8	35.7	27.1	13.4	6.7	47.0	50.2	58.3	62.3
Integrated Rain	(kT/km)	158.8	127.8	198.5	152.5	90.9	41.2	246.7	248.3	269.3	245.2
Peak Hailfall	(mm)	11.7	3.6	26.7	8.8	0.8	1.6	3.4	3.0	1.4	0.6
Integrated Hail	(kT/km)	47.9	15.7	66.0	32.1	2.4	5.4	6.5	7.1	3.7	1.2
Integrated Vapor Flux	(kT/km)	955.0	971.4	1998.0	2002.3	1547.4	1381.5	1761.6	1615.6	2015.4	2024.5
Precipitation Efficiency	(%)	21.6	14.8	13.2	9.2	6.0	3.4	14.4	15.8	13.5	12.2

development of clouds occurring in the High Plains region where the primary precipitation formation mechanism follows the development of ice in the form of snow and graupel. In the southeastern United States, it is known that the initial production of precipitation occurs through a coalescence process which can be followed by the additional formation of precipitation through the formation of ice as the cloud grows into regions where the temperature is colder than 0°C. Thus the storms of COHMEX present a somewhat different environment for the evolution of their electrical structure than do those of the High Plains. The model had previously shown some skill in the capacity to predict the electrification of High Plains storms. The present study provided the opportunity to test the efficacy of the model in a different microphysical environment.

The 20 July case was simulated because it was the most thoroughly documented of the storms during the field project. However, the electrical observations on this storm were rather sparse, consisting of observations of intracloud and cloud-to-ground lightning and one instrumented balloon launch during the dissipating stage (Goodman et al., 1988). Because the SEM in its current configuration is only capable of simulating storm development up to the stage of first lightning (no lightning discharge is included), the electrical observations provide a very limited basis for electrical comparisons. Essentially, they provide a means of determining the stage of development of the storm at the time of first lightning when used in conjunction with radar data which, for this storm, gave a detailed history of its dynamic and, to a lesser degree, microphysical evolution.

The SEM is a hybrid version of the 2D bulk water model described above and used in the analysis of Tuttle et al. (1989). The 2D model was modified by Helsdon et al. (1984) to include electrical variables and processes such as the presence of small ions, the horizontal and vertical electric field components, and the charging of hydrometeors by inductive (field dependent) and noninductive (field independent) interactions as well as by ion attachment. The boundary conditions used in the SEM differ from those used in the nonelectrical simulations, so the resulting cloud development differed somewhat from that reported by Tuttle et al. (1989). A detailed comparison between the model simulation and the available observations was carried out by Addison (1990).

He found that the initial precipitation formation occurred by a coalescence process, but as the cloud developed vertically past the melting level and entered its rapid growth phase, accretion-freezing dominated in the formation of precipitation. This agreed with the inferences drawn by Tuttle et al. (1989) based on their analysis of the multiparameter radar data. Thus, we concluded that the SEM was forming precipitation in a manner similar to the actual storm on 20 July, although the model seemed to produce graupel much earlier than the storm based on the interpretation of Z_{DR} measurements from the CP-2 radar.

The dynamic development of the simulated storm did not agree with the observations as well as the microphysical aspects just noted. The early dynamic development in the model was more vigorous than that observed. In addition, the model produced a microburst early in the life cycle of the storm, whereas the observations reported a microburst at the beginning of the dissipating stage. A rapid growth period occurred in both the simulation and the observations. In this case, the rapid growth occurred over an 8-min period for the observed storm while it lasted 15 minutes in the simulation. The observed storm reached a maximum height of 13.3 km AGL,

while the simulated storm ascended to 14.6 km. In comparing 71 features between the storm and the simulation, Addison found that 69% of these features represented fair to good simulations by the model.

In looking at the electrical evolution, Addison found four parameters that lent themselves to comparison between the model and the observed storm. Of these, two agreed well and two did not. The time of the first lightning was 14:09:30 CDT which compared poorly to an estimated time of 14:20 in the model simulation. Also, the observations indicated that first lightning occurred only 4 minutes after the formation of significant hail as inferred from the CP-2 data. In the model, breakdown electric fields (~400 kV/m) occurred some 23 minutes after the appearance of graupel. Although this comparison appears to be rather weak, it must be remembered that the inference of hail based on Z_{DR} measurements may contain significant error, and that the choice of 400 kV/m as a breakdown threshold for lightning is a very rough approximation. Thus, this comparison is very tenuous at best. On the other hand, the dynamic and electrical development during the rapid growth phase were found to correlate well, especially in that the first lightning occurred as the cloud neared its maximum height, and the strongest fields in the simulation occurred just prior to the time maximum cloud top height was reached.

Another feature that was revealed by the simulation was that the main charge centers and the associated electric field were concentrated in the upper portion of the cloud coincident with the presence of graupel, snow, and cloud ice. In fact, only 1 km separated the centers of the positive and negative charges at the time of breakdown field strength (positive charge center at 11.6 km and negative charge center at 10.6 km AGL). This concentration of charge in the upper part of the cloud resulted in the strong electric field region being concentrated in the upper portion of the cloud. These aspects are illustrated in Fig. 5. Based on this charge and field structure, we would infer that the initial breakdown would be of an intracloud nature and that intracloud lightning would continue to occur until there was significant transport of charge to lower altitudes in the cloud, either by lightning itself or by the fall of charged precipitation. The lightning observations for this storm reported by Goodman et al. (1988) reveal that out of 116 total flashes, 110 were intracloud in nature and only 6 were cloud-to-ground.

Although the SEM simulation of the 20 July COHMEX storm was disappointing in some respects, we conclude that the electrification of the storm was a result of the interaction of graupel with snow and cloud ice in a riming environment. The exact nature of the charge separation process cannot be determined from the simulation because of a recently discovered conceptual error in the implementation of the non-inductive charging process. Despite the inherent differences between the thunderstorms of the southeast and the High Plains, it seems that the interactive charging of ice particles is best able to explain thunderstorm electrification in both regions. Futher runs are necessary to distinguish between the abilities of the inductive versus the non-inductive charging mechanisms in accounting for the charging of these storms. At present, we are adjusting the boundary conditions of the SEM to agree with the model of Tuttle et al. (1989), which produced a better simulation of the storm, including the time of the microburst. If we can duplicate these results, we can apply the corrected version of the SEM (noninductive charging fixed) to the case to make a determination of the efficacy of the two primary charging processes.

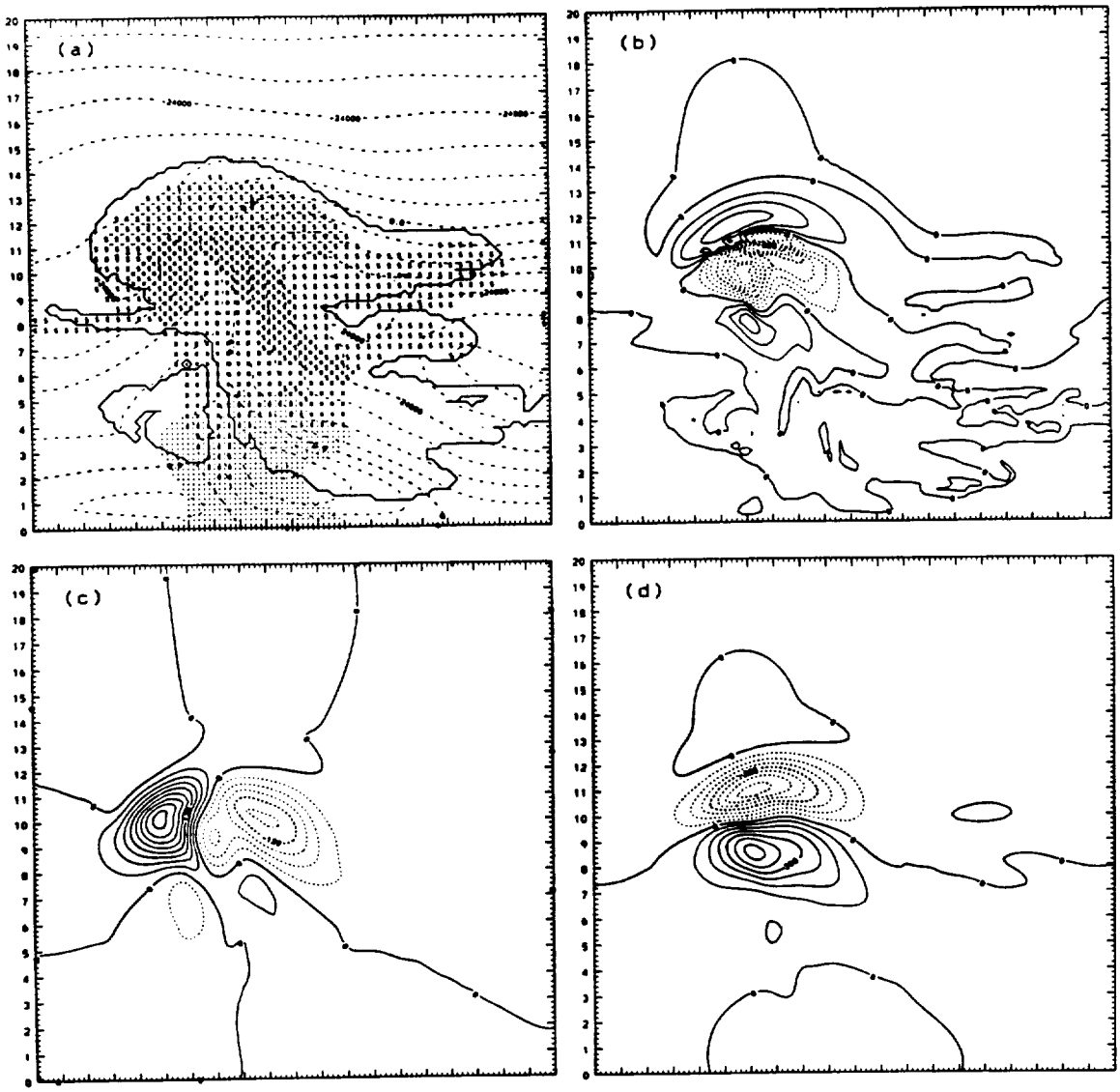

Fig. 5: Results of the storm electrification model for the 20 July COHMEX case just prior to exceeding the discharge threshold. (a) Depiction of the cloud and precipitation fields. The cloud outline is indicated by the sold line, dots and asterisks indicate rain and graupel/hail, respectively, greater than 1 g kg^{-1} and snow and cloud ice greater than 0.5 g kg^{-1} are indicated by S's and minus signs respectively. Dashed contours are for the stream function using a contour interval of 6000 kg m^{-1} s^{-1}. (b) The total charge density field; contours range from -6.4 to 2.4 nC m^{-3} with a contour interval of 0.8 nC m^{-3}. Dashed lines indicate negative values and solid lines indicate positive values. (c) The horizontal electric field; contours range from -150 to 240 kV m^{-1} with a contour interval of 30 kV m^{-1}. (d) The vertical electric field; contours range from -350 to 300 kV m^{-1} with a contour interval of 50 kV m^{-1}.

REFERENCES

Addison, R. V., 1990: Early thunderstorm electrification and comparison of model results with observations of the 20 July 1986 COHMEX storm. M.S. Thesis, Department of Meteorology, SD School of Mines and Technology, Rapid City, SD. 140 pp.

Goodman, S. J., D. E. Buechler, P. D. Wright and W. D. Rust, 1988: Lightning and precipitation history of a microburst-producing storm. Geophys. Res. Ltrs., 15, 1185-1188.

Helsdon, J. H., Jr., and R. D. Farley, 1987a: A numerical modeling study of a Montana thunderstorm. 1. Model results versus observations involving nonelectrical aspects. J. Geophys. Res., 92, 5645-5659.

Helsdon, J. H., Jr., and R. D. Farley, 1987b: A numerical modeling study of a Montana thunderstorm. 2. Model results versus observations involving electrical aspects. J. Geophys. Res., 92, 5661-5675.

Helsdon, J. H., Jr., R. D. Farley and H. D. Orville, 1984: A numerical modeling study of ice electrification mechanisms in a Montana cloud. Preprints 7th International Conf. Atmos. Elec., Albany, NY, Amer. Meteor. Soc., 174-177.

Kopp, F. J., and H. D. Orville, 1991: The use of a two-dimensional, time-dependent cloud model to predict convective and stratiform clouds and precipitation. [Submitted to Wea. and Forecasting]

Kopp, F. J., H. D. Orville, J. A. Jung and R. T. McNider, 1990: A parameterization of radiation heating at the surface in a numerical cloud model. Preprints Conf. Cloud Physics, San Francisco, CA, Amer. Meteor. Soc., J81-J84.

Kubesh, R. J., D. J. Musil, R. D. Farley and H. D. Orville, 1988: The 1 August 1981 CCOPE storm: Observations and modeling results. J. Appl. Meteor., 27, 216-243.

Tuttle, J. D., V. N. Bringi, H. D. Orville and F. J. Kopp, 1989: Multiparameter radar study of a microburst: Comparison with model results. J. Atmos. Sci., 46, 601-620.

3. PROJECT BIBLIOGRAPHY

3.1 Papers in Refereed Journals

Tuttle, J. D., V. N. Bringi, H. D. Orville and F. J. Kopp, 1989: Multiparameter radar study of a microburst: Comparison with model results. J. Atmos. Sci., 46, 601-620.

Orville, H. D., R. D. Farley, Y-C. Chi and F. J. Kopp, 1989: The primary cloud physics mechanisms of microburst formation. Atmos. Res., 24, 343-357.

Kopp, F. J., and H. D. Orville, 1991: The use of a two-dimensional, time-dependent cloud model to predict convective and stratiform clouds and precipitation. [Submitted to Weather and Forecasting]

3.2 Papers in Conference Preprint Volumes

Orville, H. D., F. J. Kopp, R. D. Farley and Y-C. Chi, 1988: On the microphysics of microbursts. Preprints 10th Intnl. Cloud Phys. Conf., Bad Homburg, F.R.G., 675-677.

Orville, H. D., Y-C. Chi, F. J. Kopp and R. D. Farley, 1989: On the microphysics of microbursts. Preprints 5th WMO Scientific Conf. Wea. Modif. and Appl. Cloud Physics, Beijing, China, 683-686.

Orville, H. D., D. P. Todey, R. D. Farley and F. J. Kopp, 1990: More on the microphysics and dynamics of microbursts. Preprints Conf. Cloud Physics, San Francisco, CA, Amer. Meteor. Soc., 582-588.

Kopp, F. J., H. D. Orville, J. A. Jung and R. T. McNider, 1990: A parameterization of radiation heating at the surface in a numerical cloud model. Preprints Conf. Cloud Physics, San Francisco, CA, Amer. Meteor. Soc., J81-J84.

3.3 M.S. Theses

Jung. J. A., 1989: The use of cloud models in forecasting. M.S. Thesis, Department of Meteorology, South Dakota School of Mines and Technology, Rapid City, SD. 66 pp.

Addison, R. V., 1990: Early thunderstorm electrification and comparison of model results with observations of the 20 July 1986 COHMEX storm. M.S. Thesis, Department of Meteorology, South Dakota School of Mines and Technology, Rapid City, SD. 140 pp.

3.4 Project Travel

Orville, H. D., to New Orleans, LA, 12-19 January 1991 to attend 71st Annual Meeting of the AMS, 1st International Symposium on Winterstorms, and other AMS meetings.

Kopp, F. J., and H. D. Orville to Kananaskis Park, Canada, 21-26 October 1990 to attend 16th Conference on Severe Local Storms, 8th Conference on Hydrometeorology, and Conference on Atmospheric Electricity.

Orville, H. D., to Denver, CO, 10-13 October 1990, to attend 7th Biennial Meeting of Heads and Chairpersons of Departments of Atmospheric and Oceanographic Sciences and attend WMA meeting.

Helsdon, J. H., to Tallahassee, FL, 26-30 March 1989, to attend 24th Conference on Radar Meteorology and chair session.

Helsdon, J. H., to Huntsville, AL, 15 July-7 August 1988, to visit NASA to discuss research results.

Orville, H. D., and J. H. Helsdon to Huntsville, AL, 12-16 December 1987, to attend COHMEX Workshop and Review Meeting.

Kopp, F. J., to Huntsville, AL, 4-23 August 1987, to work on NASA modeling projects on NASA's computer system.

3.5 Project Personnel

Addison, Roy
Farley, Richard D.
Helsdon, John H.
Jung, Jim
Kopp, Fred J.
Palmer, Sandra
Orville, Harold D.
Robinson, Joie L.
Vande Bossche, Carol L.